Materials Science in Semiconductor Processing 66 (2017) 99–104

Contents lists available at ScienceDirect

Materials Science in Semiconductor Processing

journal homepage: www.elsevier.com/locate/mssp

Lifetime improvement in silicon wafers using weak magnetic fields

A. Kuryliuk*, L. Steblenko, A. Nadtochiy, O. Korotchenkov

Faculty of Physics, Taras Shevchenko Kyiv National University, Kyiv 01601, Ukraine

ARTICLE INFO

Keywords:
Silicon
Point defects
Magnetic field

ABSTRACT

We improve the lifetime of *n*-type Czochralski-grown silicon wafers using weak magnetic fields. This processing is found to increase carrier lifetimes by up to a factor of 2, from about 3 μs to 7 μs in our samples. Employing atomic and magnetic force microscopy, surface photovoltage transients, and X-ray photoelectron spectroscopy technique, we show that the effect can be explained by the magnetic field stimulated impurity diffusion from a bulk into the crystal surface, which forms impurity nanoclusters on the surface that can serve as centers of absorption of chemical elements from the environment. This, in turn, increases the oxide film thickness. We furthermore assume that the growth of SiO_2 leads to negatively charged oxygen species in the vicinity of the Si/SiO_2 interface. The existence of a local electric field generated by the charged areas can thus cause surface gettering by the positively charged metal ions, such as K^+, Na^+, Ca^+, Al^+, moved from the wafer bulk. Exposure to weak magnetic fields is therefore assumed to be important for the cost effective overall gettering efficiency during processing of silicon wafers for solar cell production.

1. Introduction

Czochralski-grown silicon (Cz-Si) is the mostly important base material for different photovoltaic (PV) and microelectronic technologies [1]. The PV technology has attracted much attention due to clean energy conversion, reliability and infinite abundance of light energy with a comparatively easy installation process [2,3].

The cell efficiency has been gradually improved to a value smaller than ≈25% [4–6], with the theoretical limit of about 29% by solely considering the radiative recombination channel as required by the principle of detailed balance [7]. The conversion efficiency of the Si solar cell can be related to several loss factors such as the ratio of electrons that are not excited to the conduction band per incoming photon, which is often referred to as the optical loss, and that excited to the conduction band but not delivered to outer circuits, which represents the electrical loss [8]. Furthermore, the electrical loss can be further classified into several types, including the loss due to electron-hole recombination as well as scattering of the carriers.

It was long believed that *p*-type Si solar cells were superior to the *n*-type cells [9], have high throughput and can thus dominate the PV industry. Since *p*-type wafers are widely available, their price is cheaper than that of *n*-type wafers. Moreover, the electron mobility in the *p*-type wafers was higher than that in the *n*-type Si. Meanwhile, *p*-type Si has low minority carrier lifetime and light-induced degradation [9], so that high efficiency Si solar cells, such as passivated emitter with rear locally diffused (PERL), heterojunction (HIT) and interdigitated back contact (IBC) solar cells, are made on *n*-type wafers [10]. Of particular importance for demanding structures like IBC solar cells is a documented increase in minority carrier lifetime in *n*-type wafers in comparison with the lifetime observed in *p*-type wafers [11,12]. Further proof of importance in terms of the PV industry is that the *n*-type wafer has higher tolerance to impurities [9].

The minority carrier lifetime is a reliable indicator of the wafer quality. Doping with impurities and high-temperature heat treatments always tend to reduce the minority carrier lifetime. Some types of impurities and defects can be removed from the bulk of a wafer by gettering mechanisms [11], which might improve the lifetime.

The gettering processes redistribute impurities in a specific region of a wafer, e.g. at the surfaces, which can then be either removed by etching, or isolated from the active device regions. In the first case, appropriate techniques are referred to as "extrinsic" gettering. Common examples in Si include metal film deposition, solute diffusion, mechanical or laser damage, ion implantation, polysilicon deposition, corona discharge, Ge-doped Si epitaxy, chlorine or sacrificial oxidation, deposition of Si_3N_4 film or porous silicon layer [13]. In contrast, the techniques exploiting internal features such as dislocations, grain boundaries, oxygen precipitates or micro-defects are known as "intrinsic" gettering. This is commonly used in microelectronics and information technology (IT) industry [14–16] where a large portion of the wafer is electronically isolated from the device, a situation that rarely occurs in solar cells.

In the last decade, new approach to controlling electronic processes

* Corresponding author.
E-mail address: kurylyuk_a2008@ukr.net (A. Kuryliuk).

http://dx.doi.org/10.1016/j.mssp.2017.03.032
Received 13 December 2016; Received in revised form 14 March 2017; Accepted 30 March 2017

in semiconductors has been proposed based on the application of magnetic fields. Recently, much research has been devoted to magnetic-field assisted change in the electronic properties of silicon wafers and nanostructures [17–22]. Exposure to magnetic fields can be a cost-effective solution for making silicon an ideal solar-grade and electronic-grade material for microelectronic fabrication facilities. Using a pulsed magnetic field was proven significantly affecting the surface relief profile of Si wafers. Thus, the roughness of the wafer surface can increase significantly, from about 1.3–5.8 nm, as reported by Levin et al. [17].

Despite particular achievements in this field very little is known about the nature of the accompanying effects. In particular, the definite experimental evidence for the involvement of trapping and recombination centers is still lacking and some of the results are largely incomplete and controversial.

The aim of this paper is to present a new method for enhancing the lifetime of silicon wafers. We suppose that exposure to magnetic field speeds up the defect reactions in silicon with a subsequent modification of the subsurface structure. The resulting occurrence of electric fields can cause surface gettering by charged ions moved from the wafer bulk.

2. Experimental

The experiments were performed using both an electronic grade silicon, which was used to fabricate semiconductor chips, and a solar grade low-quality monocrystalline silicon, originating from impure Czochralski ingots. The wafers obtained with standard Cz technique had double-side-polished surfaces. The Si(111) wafers were phosphorus doped to the resistivity of 4.5 Ω cm, having the thickness of ≈500 μm and 1–3 nm thick native oxide on their surface. The concentration of transition metals, such as Cu, Fe, Au, in the wafers approached 10^{16} cm^{-3}, as determined by secondary ion mass spectroscopy (SIMS) from the depth of a few microns inside the wafer.

Magnetic treatments (MT) of Si wafers were performed by placing the samples in a static magnetic field B_0 oriented along the normal to the wafer surface and produced by ferromagnetic plates. The strength B_0 was varied from 0.1 to 0.35 T by changing the distance between the poles. The wafers were kept in the measured cell at ambient conditions for more or less prolonged times. For each set of MT conditions, three to five pairs of sister wafers were used. The data from the treated samples and from the control samples were each averaged to produce two data points, one for MT and one for the reference. It was previously reported that, varying both the strength of magnetic fields and the length of time when the field was applied, the field-induced changes in various silicon parameters saturate at $B_0 \approx 0.2$ T and the magnetic treatment time t_{MT} ranging from 7 to 10 days [23,24]. Keeping all of these considerations in mind, here we restruct our consideration to the lifetime effects observed at $B_0 = 0.17$ T and $t_{MT} = 7$ days.

Atomic force microscopy (AFM) and magnetic force microscopy (MFM) measurements were performed under ambient conditions using a commercial instrument (NT-MDT NTEGRA Prima Scanning Probe Microscope). The topographic and magnetic images were obtained using the two-pass (tapping/lifts mode) technique [25]. In the first pass, the surface profile was imaged in the tapping (intermittent contact) mode [26]. The magnetic structure of the sample surface was mapped in the second pass, when the magnetic sensor tip scanned the previously measured topographic profile at an adjusted distance (lift-height) in the range from 10 to 100 nm above the wafer surface. The magnetic image was obtained by measuring the phase shift of vibrating cantilever at its first flexural resonance, which varied with changing the magnetic tip–sample interaction forces. The tip-sample magnetic interactions were therefore used to reconstruct the magnetic structure of the sample surface.

Surface photovoltage (SPV) transients were measured in the capacitor arrangement using a red light-emitting diode as an excitation source. Details of our setup are given elsewhere [27]. A parallel plate capacitance was formed between a metal grid electrode and the wafer, separated by a mica insulating foil with a thickness of about 20 μm. A 1 GΩ load resistor, a high-impedance buffer cascade based on a field-effect transistor and a sampling digital oscilloscope were used in the measurements. The scanning SPV setup, which provides wafer maps of both the SPV magnitude and decay time with a 100 μm spatial resolution, was discussed by Nadtochiy et al. [28]. A sequence of SPV transients was averaged up to 10^4 times.

X-ray photoelectron spectra (XPS, EC-2402 spectrometer) were recorded using a monochromatic Mg Kα radiation (energy 1253.6 eV, X-ray source power 200 W), an energy analyzer PHOIBOS-100-SPECS, an ion source IQE 11/35 and a Flood Gun FG 15/40 for compensating the surface charge. The energy resolution of the analyzer was set to 0.1 eV. The X-ray penetration depth was $\approx 10^5$ нм at a photon energy ranging from 1.2 to 1.5 keV. The data were acquired with photoelectron escape depths ranging from 2 to 5 nm at the kinetic energy varying from 1 to 2 keV. Individual Si 2*p* peak components with the full width at half maximum (FWHM) of 1.2 eV in Si and 1.5 eV in SiO_2were decomposed using a Gauss-Newton method. The background was subtracted from the raw XPS signal using the method described by Shirley [29].

3. Experimental results and discussion

In our experiments, a weak external dc magnetic field with $B = 0.17$ T was applied to Si crystals during $t_{MT} = 7$ days, and the

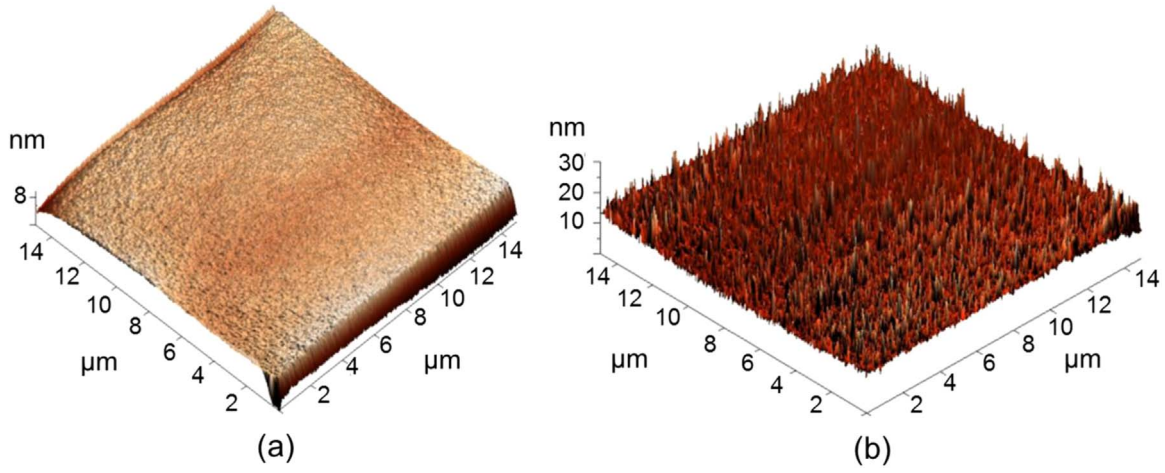

Fig. 1. AFM images of the same *n*-Si surface taken before (*a*) and just after (*b*) MT with $B_0 = 0.17$ T during $t_{MT} = 7$ days.

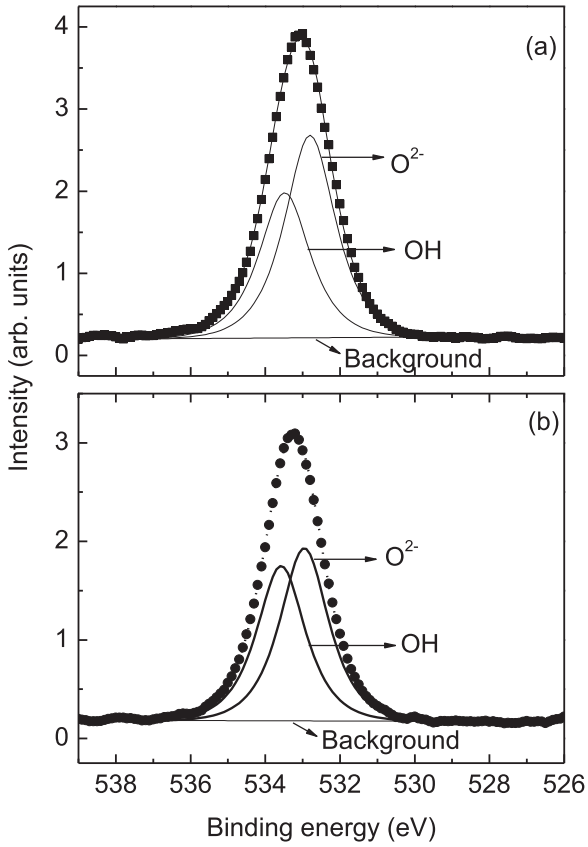

Fig. 2. Measured and fitted O1*s* XPS spectra of the unprocessed wafer (a) and the one just after MT with $B_0 = 0.17$ T during $t_{MT} = 10$ days (b). Sum of the O^{2-} and OH components (solid lines) is given by dotted lines.

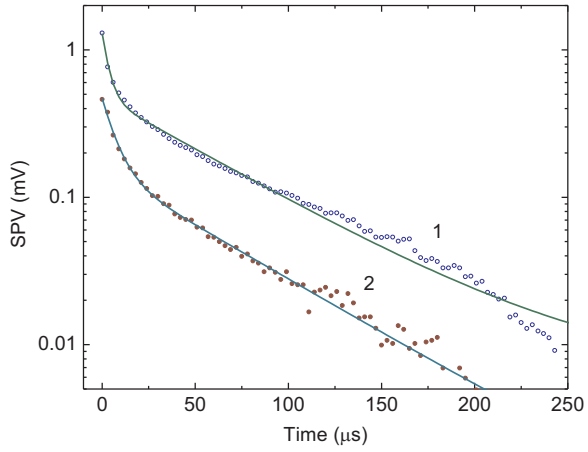

Fig. 3. Representative time-dependent SPV (after the LED light was off) of an unprocessed wafer covered with native oxide (1) and the one after MT (2) with $B_0 = 0.17$ T during $t_{MT} = 7$ days. Points – experiment, line – best fits to Eq. (1) with parameter values $V_1 = 1.28$ mV, $V_2 = 0.48$ mV, $\tau_1 = 3.63$ μs, $\tau_2 = 60.68$ μs for curve 1 and $V_1 = 0.34$ mV, $V_2 = 0.15$ mV, $\tau_1 = 7.30$ μs, $\tau_2 = 58.93$ μs for curve 2.

surface relief was checked via AFM. The main result is shown in Fig. 1, illustrating that the surface topology is obviously modified by the field such that hills and cavities of various shapes and diameters are observed after MT. From the data of Fig. 1, the roughness parameter R_a (RMS value) exhibits up to 3 times increase (from about 0.4–1.2 nm) due to MT. Based on the previously reported results [17–22], this can be thought of as resulting from the magnetic field stimulated impurity diffusion from a bulk into the crystal surface, which mounts impurity nanoclusters on the surface.

Our MFM studies revealed 6 times increase in the interaction force between the sample surface and cantilever. This fact shows that, first, the surface of the dislocation-free silicon is enriched with magnetic-sensitive impurities and, second, the impurities migrating from a bulk into the surface not only change its topology but also turn it into the magneto-active state.

We have also tested the Si wafers containing increased dislocation density in a subsurface layer. It has been found that the impurity gettering and surface activation with magnetic field are even more pronounced in the dislocation samples. This observation can be understood as being due to the fact that dislocations, like surfaces, act as strong sources of impurity gettering. This results in increased impurity flux towards the surface in the samples with high dislocation densities. Noticeably, the MT modified Si surface, left in a state of rest for about 60 days, relaxes to nearly initial state and the impurity gettering-induced topology changes almost completely disappear.

Therefore, there remains the possibility that the nanoclusters, which are formed on the surface of the wafer and revealed by AFM, can serve as centers of absorption of chemical elements from the environment. This, in turn, increases the oxide film thickness.

The O 1*s* XPS spectra of the unprocessed and MT wafers are contrasted in Fig. 2, a and b. The two individual peaks in the deconvoluted spectra are attributed to O^{2-} and OH components. The observed increase in the OH component can be due to increased concentration of silicon hydrogenated clusters after MT.

The time-resolved SPV responses of one of our samples are displayed in Fig. 3. For MT samples, all transients show more or less slowing down initial parts of the decay (curve 2 compared with curve 1), which depends on the detection point on the wafer surface as well as on the time of rest after the field is turned off. Then the transient SPV tails off with a relatively gentle slope (see after 20–30 μs in Fig. 3), which also varies across the wafer surface.

The transients cannot be generally described by a single exponential but rather can be well fitted to the two-exponential time decay,

$$V(t) = V_1 \exp(-t/\tau_1) + V_2 \exp(-t/\tau_2), \quad (1)$$

as exemplified by curves in Fig. 3. As a consequence, we can suggest an involvement of at least two distinct processes forming SPV. It may therefore be assumed that the two-exponential decay of excess charge carriers in the wafers can be understood based on a model that couples surface carrier dynamics with transport in the surface band bending layer.

It is worth noting at this point that crystalline Si usually contains a variety of defects ranging from various point defects to extended defects, such as microdefects or second phase precipitates, dislocations, grain boundaries. The electrical performance of silicon, e.g. its minority carrier lifetime, is closely related to metal impurities present in the feedstock or introduced during crystal growth [30,31].

It is also worthwhile noting that the charge on hydrogenated Si surfaces and its dependence on the surface morphology was thoroughly addressed previously [32,33], which forms the basis for relating our SPV results to the local surface roughness of MT wafers given above. As reported by Dittrich et al. [33], the smoothest surface should be completely free of surface states, whereas a well-facetted hydrogenated surface has a relatively large number of surface atoms at steps and corners. The bonds are weaker at such sites and the probability for surface chemical transformations and adsorption of molecules is increased. The presence of fast electronic surface states on MT Si surfaces would therefore lead to relatively high surface recombination velocities, thus accelerating SPV decays.

The latter also increases the roughness parameters, which can be associated with the magnetic field stimulated diffusion of impurities towards the sample surface and thus the formation of impurity nanoclusters capable of affecting the surface topography. This kind of gettering effect elucidated by MT induced enrichment of the surface

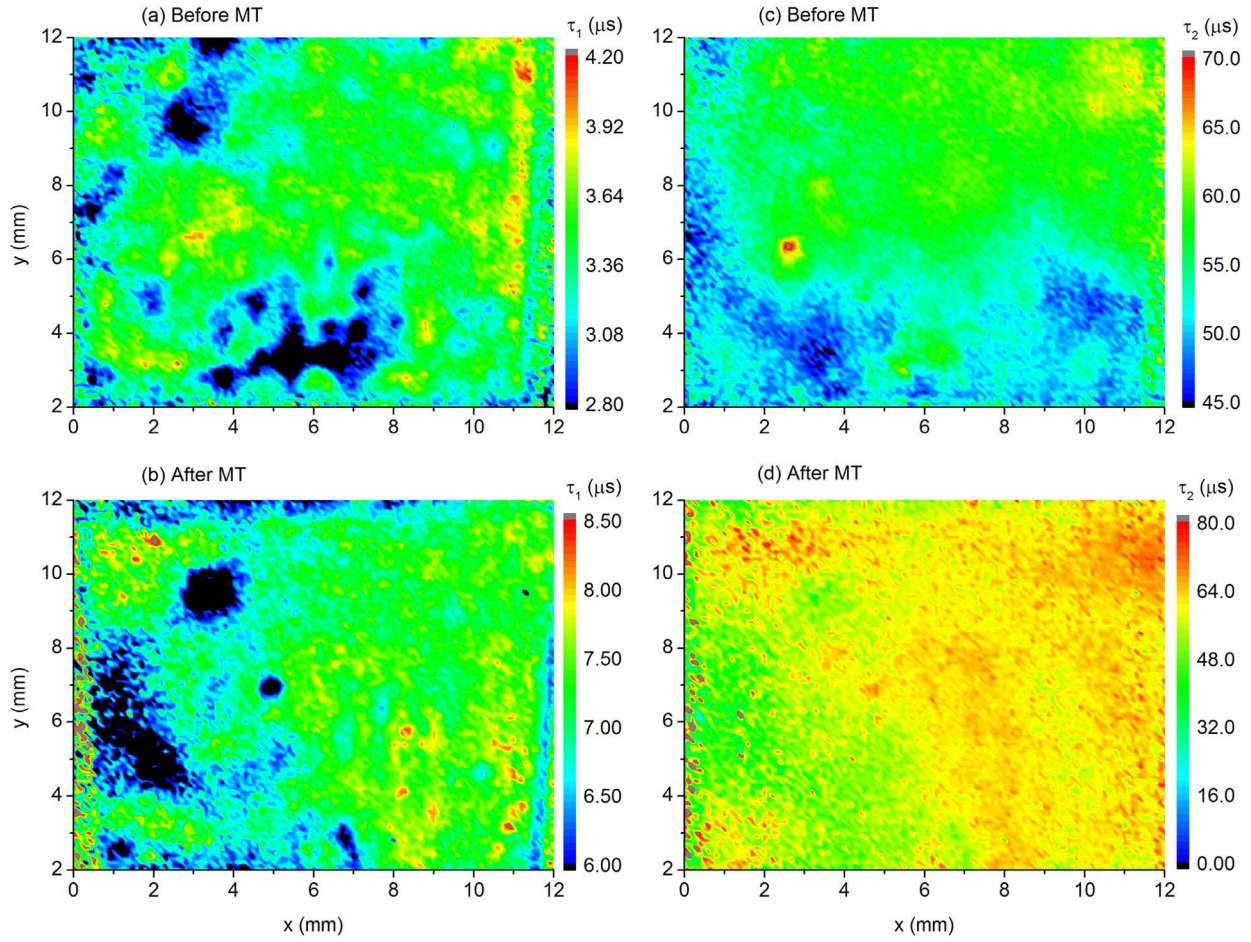

Fig. 4. Distributions of τ_1 and τ_2 in Eq. (1) across the surface of native oxidized Si wafer before (a and c) and after (b and d) MT with $B_0 = 0.17$ T during $t_{MT} = 7$ days.

with impurities expelled from the bulk is also supported by the magnetic force microscopy data.

It is well known that electronic processes in semiconductors are related to chemical processes occurring on their surface [34]. Surface defects can act as active centers of adsorption and catalysis, causing the semiconductor surface to charge up. The charge state of the defect is of paramount importance for the adsorption, as the adsorption rate is quite different for charged and neutral defects.

One can therefore assume that in the process of MT induced saturation of surface dangling bonds the selective adsorption of oxygen (as the most active adsorption component) leads to local negatively charged surface areas. The existence of a local electric field generated by the charged areas can thus cause surface gettering by the positively charged ions of alkali metals moved from the wafer bulk.

This conclusion is supported by appropriate SIMS data given by Koplak et al. [23]. Indeed, samples that underwent MT processing generally showed an improvement in the gettering efficiency of some light and positively charged ions relative to control samples for both top and bottom surfaces of the wafers.

It is therefore possible to imagine the occurrence of recombination centers and traps among the subsurface centers affected by MT, which in turn affect the SPV response. The presence of rapid surface states on Si surfaces would accelerate the surface recombination that speeds up the SPV decays, while gettering metal impurity is helpful to raise the lifetime of the wafer. To find a spatial distribution of the decay times, the SPV mapping was performed.

The spatially distributed τ_1 and τ_2 (see Eq. (1)) in the wafer before and after MT is shown in Fig. 4. The areas shown in red and blue have the lowest and highest decay time, respectively. The maps give a spatially inhomogeneous decay time, which is most likely to correlate with the distribution of aggregated impurities, adsorbed molecules and the dislocation density of different regions of the material.

It is clearly seen in Fig. 4 that the measured τ_1 and τ_2 seem to exhibit greater effective values after MT. The effective lifetime can then be given by

$$\frac{1}{\tau} = \frac{1}{\bar{\tau}_1} + \frac{1}{\bar{\tau}_2}, \tag{2}$$

where $\bar{\tau}_1$ and $\bar{\tau}_2$ are the decay times estimated by averaging τ_1 and τ_2, respectively, over the entire area of the wafer surface mapped in Fig. 4. This yields the lifetime values of $\tau = 3.1$ and 6.5 μs before and after MT, respectively. This increase in the lifetime is a supporting evidence of the metal impurity gettering.

The probability of occurrences of particular values of V_1, V_2, τ_1 and τ_2 is displayed in Fig. 5. It is seen that, just after MT is turned off, the values of V_1 and V_2 in Eq. (1) are unevenly distributed across the surface. Moreover, their distributions shift to smaller values of V_1 and V_2 peaked at 0.1–0.2 mV (curves 2 in Fig. 5,a and b) with respect to the ones reproduced in an unprocessed wafer peaked at 0.2–0.4 mV (curves 1 in Fig. 5,a and b). Such charge neutralization at recombination centers both on the surface and in the subsurface layer can be due to the occurrence of defect interactions with the charged recombination centers, which are present in unprocessed wafers, and impurities adsorbed at the surface during MT.

The adsorption process, which is accelerated at the MT surface, generates additional energy levels in the crystal. It may therefore be suggested that the charge of adsorbed impurities modifies the surface charge. Indeed, it is know that water molecules adsorbed on the surface of silicon form both donor and acceptor levels while adsorbed oxygen forms acceptor levels [34]. To our mind, this can partially neutralize

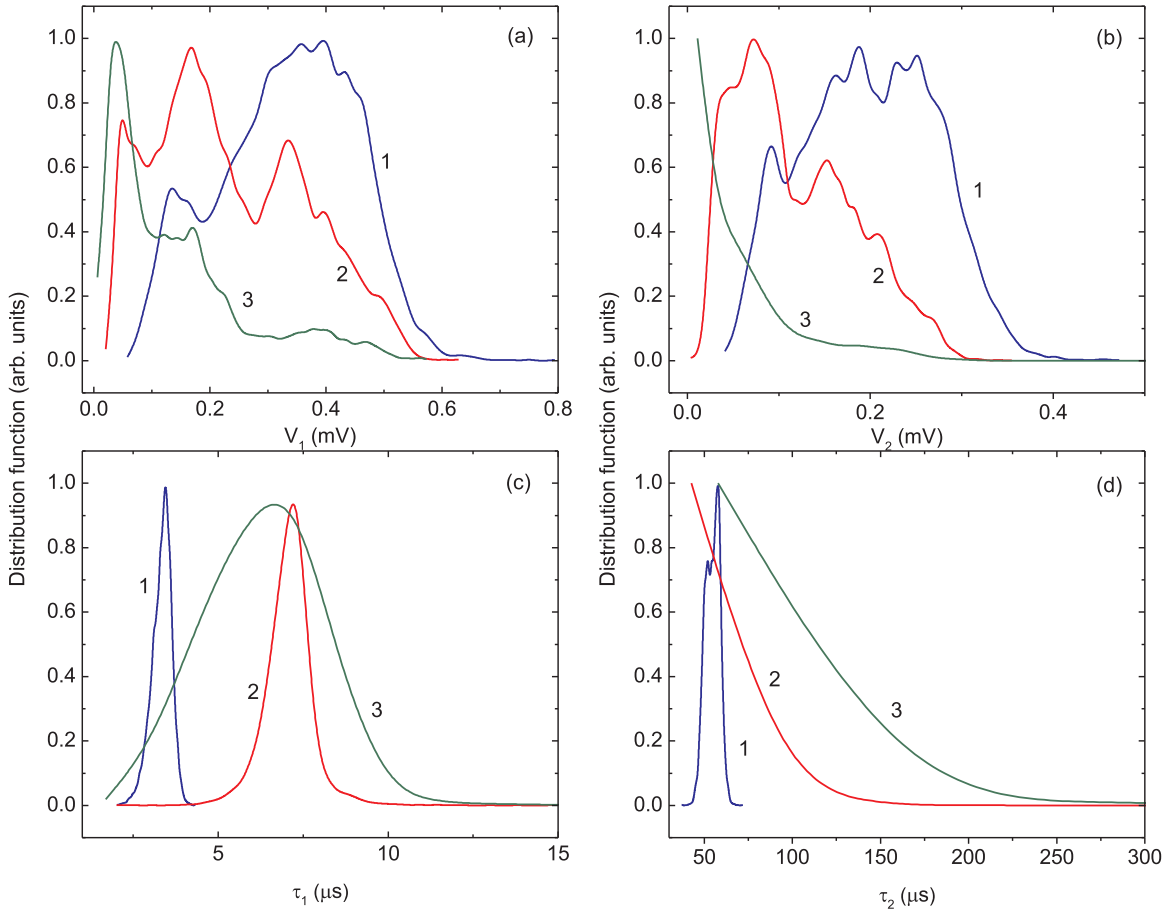

Fig. 5. Probability of occurrences of particular values of V_1, V_2, τ_1 and τ_2 in Eq. (1) in unprocessed wafer covered with native oxide (1), the one after MT with $B_0 = 0.17$ T during $t_{MT} = 7$ days (2) and 7 days after the treatment was turned off (3).

charged surface centers and explain the relaxation effect after MT is turned off,-particularly, the increased and broader distributed carrier lifetimes seen in curves 3 compared with curves 1 and 2 in Fig. 5c and d.

The properties of materials are mainly characterized by the motion of electrons, which interact with a magnetic field through the magnetic moment caused by spin- and orbital-angular momenta, or cyclotron motion caused by the Lorentz force. Therefore, it is quite common to believe that the material can respond to an applied magnetic field, as widely discussed in the literature [35]. The magnetic field is one of the thermodynamic parameters that are used to change the inner energies of materials, along with temperature and pressure. However, the effect of a magnetic field on materials is small compared with the effects caused by other parameters. For example, a 10 T field corresponds to the density of 4×10^7 J m^{-3}, while the interaction energy at 10 T is only about 2×10^{-22} J [35].

In magnetic materials, a variety of phase transitions can be induced using an applied magnetic field, according to the theoretical descriptions of both the classical and quantum mechanical approaches. In diamagnetic materials, magnetic moments caused by spin- and orbital-angular momentum in an atom or a molecule compensate each other such that there is no net magnetic moment. Even these materials respond to a magnetic field via Larmor diamagnetism, which is due to the orbital motion of electrons; this is induced by the magnetic field according to Lenz's law. In this case, however, the effects of the magnetic field are very small, typically three orders of magnitude smaller as compared to that observed in electric conductors or magnetic materials.

In general, the interactions increase strongly with increasing field, and more detailed properties of materials are revealed macroscopically and microscopically. In other words, we can obtain more information about materials via the Zeeman and/or Landau energies, resulting from measurements in higher magnetic fields. Meanwhile, the limit of relatively low magnetic fields has been given small attention.

The above results can be understood in terms of increased chemical activity of silicon crystal surface exposed to magnetic fields, whereas in the absence of magnetic field the surface is quite inert. From our experiments, it is enhanced defect concentration on the sample surface that is most likely responsible for this increase.

Different mechanisms behind the magnetic-field increased chemical activity have been so far addressed, such as spin dependent surface reactions involving unstable intermediate Si–O–Si complexes as precursors [23], triplet–singlet spin conversion that transforms the oxygen molecules in the triplet spin states into the reactive singlet states [24], etc. On the other hand, the silicon oxidation process is generally assumed to occur sequentially through (i) the O_2 diffusion through the oxide network toward the Si/SiO_2 interface and (ii) an activated O_2 reaction with the Si substrate at the interface [36]. Furthermore, ionic and neutral oxygen species, both molecular and atomic, introduced into amorphous SiO_2 change significantly the energetics of defect processes like charge state change [37].

Yet it must with be kept in mind that, in the vicinity of the Si/SiO_2 interface, electrons can tunnel from the silicon substrate to the approaching O_2 molecule giving rise to negatively charged oxygen species [37]. In accord with the underlying assumption mentioned above, this localization of the excess negative charge near the Si/SiO_2 interface can explain the movement of the metal ions, such as K^+, Na^+, Ca^+, Al^+, towards the surface of the Si wafer.

4. Conclusion

In summary, we report that exposure to weak dc magnetic fields increases the free carrier lifetime in Si wafers, which is thought to be a convincing evidence of the metal impurity gettering effect. This processing is found to improve carrier lifetimes by up to a factor of 2, from about 3 μs to 7 μs in our wafers. Magnetic field treatment is therefore expected to have substantial impact on optimizing the gettering procedure and can be cost effective and easily incorporated into current silicon processing steps.

References

[1] J. Schmidt, K. Bothe, D. Macdonald, J. Adey, R. Jones, D.W. Palmer, J. Mater. Res. 21 (2006) 5–12.
[2] B. Parida, S. Iniyan, R. Goic, Renew. Sustain. Energy Rev. 15 (2011) 1625–1636.
[3] A.K. Pandey, V.V. Tyagi, J.A.L. Selvaraj, N.A. Rahim, S.K. Tyagi, Renew. Sustain. Energy Rev. 53 (2016) 859–884.
[4] M. Tanaka, IEICE Electron. Express 10 (2013) 20132006.
[5] M.A. Green, K. Emery, Y. Hishikawa, W. Warta, E.D. Dunlop, Prog. Photovolt.: Res. Appl. 21 (2013) 1–11.
[6] M. Taguchi, A. Yano, S. Tohoda, K. Matsuyama, Y. Nakamura, T. Nishiwaki, K. Fujita, E. Maruyama, IEEE J. Photovolt. 4 (2014) 96–99.
[7] W. Shockley, H.J. Queisser, J. Appl. Phys. 32 (1961) 510–519.
[8] S.W. Glunz, R. Preu, D. Biro, Crystalline silicon solar cells – state-of-the-art and future developments, in: A. Sayigh (Ed.), Comprehensive, renewable energy, 1 Elsevier, 2012.
[9] J.E. Cotter, J.H. Guo, P.J. Cousins, M.D. Abbott, F.W. Chen, K.C. Fisher, IEEE Trans. Electron. Devices 53 (2006) 1893–1901.
[10] D. Song, J. Xiong, Z. Hu, G. Li, H. Wang, H. An, B. Yu, B. Grenko, K. Borden, K. Sauer, T. Roessler, J. Cui, H. Wang, J. Bultman, A.H.G. Vlooswijk, P.R. Venema, in: Proceedings of the 38th IEEE photovoltaic specialists conference (PVSC), 3–8, 2012, 003004–003008.
[11] J.S. Kang, D.K. Schroder, J. Appl. Phys. 65 (1989) 2974–2985.
[12] A. Cuevas, M. Stocks, S. Armand, M. Stuckings, Appl. Phys. Lett. 70 (1997) 1017–1019.
[13] C. Zhang, S. Liu, Y. Wang, Y. Chen, Mater. Sci. Semicond. Proc. 13 (2010) 209–213.
[14] K.-W. Lee, J.-C. Bea, Y. Ohara, M. Murugesan, T. Fukushima, T. Tanaka, M. Koyanagi, IEEE Trans. Device Mater. Reliab. 14 (2014) 451–462.
[15] S.-W. Lee, S.-H. Lee, D.-H. Hwang, H.-B. Kang, Solid-State Electron. 76 (2012) 30–35.
[16] J.P. Gambino, S.A. Adderly, J.U. Knickerbocker, Microelectron. Eng. 135 (2015) 73–106.
[17] M.N. Levin, A.V. Tatarintsev, O.A. Kostsova, A.M. Kostsov, Tech. Phys. 48 (2003) 1304–1306.
[18] K.M. Salikhov, Yu.N. Molin, R.Z. Sagdeev, A.L. Buchachenko, Spin Polarization and Magnetic Effects in Radical Reactions, Elsevier, Amsterdam, 1984.
[19] B. Ya, A.L. Zel'dovich, E.L. Buchachenko, Frankevich, Sov. Phys. Usp. 31 (1988) 385–408.
[20] V.A. Makara, L.P. Steblenko, Y.L. Kolchenko, S.M. Naumenko, O.A. Patran, V.M. Kravchenko, O.S. Dranenko, Solid State Phenom. 108–109 (2005) 339–344.
[21] M.N. Levin, B.A. Zon, J. Exp. Theor. Phys. 84 (1997) 760–773.
[22] R.B. Morgunov, Phys.-Uspekhi 47 (2004) 125–148.
[23] O.V. Koplak, A.I. Dmitriev, T. Kakeshita, R.B. Morgunov, J. Appl. Phys. 110 (2011) 044905.
[24] O. Koplak, R. Morgunov, A. Buchachenko, Chem. Phys. Lett. 560 (2013) 29–31.
[25] C. Lin, F.F. Fan, A.J. Bard, J. Electro Soc. 134 (1987) 1038–1039.
[26] Q. Zhong, D. Inniss, K. Kjoller, V.B. Elings, Surf. Sci. Lett. 290 (1993) L688–L692.
[27] A. Podolian, V. Kozachenko, A. Nadtochiy, N. Borovoy, O. Korotchenkov, J. Appl. Phys. 107 (2010) 093706.
[28] A. Nadtochiy, A. Podolian, O. Korotchenkov, J. Schmid, E. Kancsar, V. Schlosser, Phys. Stat. Sol. C 8 (2011) 2927–2930.
[29] D.A. Shirley, Phys. Rev. B 5 (1972) 4709–4714.
[30] A.A. Istratov, T. Buonassisi, R.J. McDonald, A.R. Smith, R. Schindler, J.A. Rand, J.P. Kalejs, E.R. Weber, J. Appl. Phys. 94 (2003) 6552–6559.
[31] T. Buonassisi, A.A. Istratov, M.D. Pickett, M. Heuer, J.P. Kalejs, G. Hahn, M.A. Marcus, B. Lai, Z. Cai, S.M. Heald, T.F. Ciszek, R.F. Clark, D.W. Cunningham, A.M. Gabor, R. Jonczyk, S. Narayanan, E. Sauar, E.R. Weber, Prog. Photo.: Res. Appl. 14 (2006) 513–531.
[32] H. Angermann, W. Henrion, M. Rebien, J.-T. Zettler, A. Röseler, Surf. Sci. 388 (1997) 15–23.
[33] Th. Dittrich, M. Schwartzkopff, E. Hartmann, J. Rappich, Surf. Sci. 437 (1999) 154–162.
[34] V.S. Vavilov, V.F. Kiselev, B.N. Mukashev, Defekty v kremnii i na ego poverhnosti, Nauka, Moscow, 1990 (in Russian).
[35] M. Motokawa, Rep. Prog. Phys. 67 (2004) 1995–2052.
[36] A.M. Stoneham, M.A. Szymanski, A.L. Shluger, Phys. Rev. B 63 (2001) 241304R.
[37] A. Bongiorno, A. Pasquarello, Phys. Rev. Lett. 93 (2004) 086102.